Superconductivity in Heavy Alkaline-Earth Intercalated Graphites

J. S. Kim,[1] L. Boeri,[1] J. R. O'Brien,[2] F. S. Razavi,[3] and R. K. Kremer[1]

[1]*Max-Planck-Institut für Festkörperforschung, Heisenbergstrasse 1, D-70569 Stuttgart, Germany*
[2]*Quantum Design, 6325 Lusk Boulevard, San Diego, California 92121, USA*
[3]*Department of Physics, Brock University, St. Catharines, Ontario, L2S 3A1, Canada*

(Received 29 March 2007; published 9 July 2007)

We report the discovery of superconductivity below 1.65(6) K in Sr-intercalated graphite SrC_6, by susceptibility and specific heat (C_p) measurements. In comparison with CaC_6, we found that the anisotropy of the upper critical fields for SrC_6 is much reduced. The C_p anomaly at T_c is smaller than the BCS prediction, indicating an anisotropic superconducting gap for SrC_6 similar to CaC_6. The significantly lower T_c of SrC_6 as compared to CaC_6 can be understood in terms of "negative" pressure effects, which decreases the electron-phonon coupling for *both* in-plane intercalant and the out-of-plane C phonon modes. We observed no superconductivity for BaC_6 down to 0.3 K.

DOI: 10.1103/PhysRevLett.99.027001 PACS numbers: 74.70.Ad, 74.25.Bt, 74.25.Kc, 74.62.Fj

The discovery of superconductivity in YbC_6 and CaC_6 [1,2] initiated intensive theoretical and experimental investigations [3–12] on the alkaline-earth graphite intercalation compounds (GICs). The results of the experimental studies, especially the observation of a Ca isotope effect [12], strongly favor electron-phonon (e-ph) coupling rather than exotic electronic mechanisms [3]. Recent *ab initio* electronic structure calculations prove that, in contrast to MgB_2, e-ph coupling involving electronic interlayer (IL) states becomes relevant [3] and is sufficiently strong to generate the relatively high T_c's [4,5,9]. These findings stimulated discussions on the variability of the e-ph coupling strength in different branches of the electronic and vibrational states for honeycomb layered compounds such as MgB_2, $CaSi_2$ [13], (Ca,Sr)AlSi [14], and also the hypothetical Li_2B_2 [15].

Many issues still remain open, especially about the nature of the relevant phonons. In order to modify the phonon spectrum, Ca isotope substitution [12] and hydrostatic pressure experiments [8–10] have been performed. The isotope experiments reported a surprisingly high isotope exponent for Ca, $\alpha(\mathrm{Ca}) \approx 0.5$, close to the BCS limit, suggesting a dominant role of the Ca phonons in the e-ph coupling [12]. However, *ab initio* calculations predicted similar isotope exponents ~0.25 for Ca and C, pointing to comparable contributions to the e-ph coupling from the Ca and C phonons [5]. The positive pressure dependence of T_c found for CaC_6 has been discussed in terms of phonon softening for the in-plane Ca vibrations [9,16]. Although the experimentally determined T_c's grow almost linearly with pressure, the *ab initio* calculations predicted a nonlinear increase with a reduced magnitude [9]. To resolve these discrepancies, possible anharmonic effects of the ultrasoft intercalant phonon modes or a continuous superconducting gap distribution due to anisotropic e-ph coupling have been suggested [17,18], asking for further investigations.

Another way to modify the relevant phonon modes is to vary the intercalant species and replace Ca with other alkaline-earths such as Sr or Ba. Mazin pointed out that for CaC_6 and YbC_6 the square root of the mass ratio of the intercalants is only 15% larger than the ratio of their T_c's [4]. Thus, according to this "isotope" effect argument, other alkaline-earth GICs may as well be superconducting. In fact, subsequent *ab initio* calculations predicted superconductivity for SrC_6 at 3.1 K and BaC_6 at 0.2 K [16]. In this Letter, we report the discovery of superconductivity in SrC_6 at $T_c = 1.65(6)$ K by susceptibility and specific heat measurements and the absence of superconductivity in BaC_6 down to ~0.3 K. The superconducting properties of SrC_6 as well as the *ab initio* calculations clearly demonstrate that SrC_6 can serve to bridge the two seemingly different classes of the superconducting GICs: the low-T_c alkali GICs and the newly discovered "high-T_c" systems, CaC_6 or YbC_6. Furthermore, the comparison of SrC_6 with CaC_6 provides a better insight into the unconventional nature of superconductivity in alkaline-earth GICs.

Samples of SrC_6 and BaC_6 were synthesized from pieces of highly oriented pyrolytic graphite (Advanced Ceramics, size $\approx 3 \times 1 \times 1$ mm^3) and Sr (99.95%) or Ba (99.95%) metal by a vapor phase reaction performed for more than a month at 470 and 500 °C, respectively. X-ray diffraction patterns show neither the signature of pristine graphite nor a mixture with higher-stage intercalated phases, indicating good sample homogeneity. The graphite layer distance increases from CaC_6 (4.50 Å) to SrC_6 (4.95 Å) and to BaC_6 (5.25 Å) as expected from the size of the intercalant atoms. The stacking sequence of SrC_6 and BaC_6 is found to be of the $A\alpha A\beta A$ type (space group $P63/mmc$) [19], which differs from the $A\alpha A\beta A\gamma A$-type stacking in CaC_6. Superconductivity for SrC_6 was first observed by ac magnetic susceptibility (119 Hz) measurements to 0.3 K and subsequently confirmed by specific heat measurements using a physical property measurement system ^{3}He calorimeter (Quantum Design). The pressure dependence of T_c was measured up to ~1 GPa as described in detail elsewhere [9]. In order to understand the superconducting properties of SrC_6 and compare with those of CaC_6, we also performed *ab initio* calculations of the

electron-phonon properties for SrC_6 using the experimental $\alpha\beta$ stacking [20,21].

Figure 1 shows a sharp superconducting transition in the magnetic susceptibility $\chi(T)$ at $T_c = 1.65(6)$ K in SrC_6. The transition width $\Delta T_c \approx 0.06$ K was determined as the temperature difference between 10% and 90% of the diamagnetic shielding. In a magnetic field, T_c shifts to lower temperatures, and the superconducting transition broadens. In BaC_6, we cannot find any signature of superconductivity down to 0.3 K. The upper critical fields $H_{c2}^{\parallel,\perp}$ for H parallel and perpendicular to the c axis follow the Werthamer-Helfand-Hohenberg (WHH) prediction rather well [23] [Fig. 1(b)]. A slight deviation from the WHH curve is found at low temperatures, which has been observed in other GICs such as CaC_6 and KC_8 [24]. Within the scope of the WHH approximation, we obtained $H_{c2}^{\parallel}(0) \approx 138$ Oe and $H_{c2}^{\perp}(0) \approx 276$ Oe as well as the corresponding coherence lengths $\xi_{ab}(0) \approx 1510$ Å and $\xi_c(0) \approx 700$ Å. Similar to CaC_6, $\xi_c(0)$ and $\xi_{ab}(0)$ are larger than the out-of-plane and the in-plane lattice constants, indicating three-dimensional superconductivity.

Bulk superconductivity in SrC_6 is confirmed by specific heat (C_p) measurements. The characteristic C_p anomaly at $T_c = 1.65$ K is clearly observed at $H = 0$ and completely disappears with $H = 500$ Oe [$H > H_{c2}(0)$]. There is no offset of C_p/T at $H = 0$ as $T \to 0$ K, indicating a complete superconducting phase. Similar to CaC_6, the normal state C_p deviates slightly from a T^3 dependence (the inset in Fig. 2), due to low-lying Einstein phonon modes. The normal state C_p can well be described by $C_p(T) = \gamma_N T + C_{\rm ph}(T)$, where γ_N is the Sommerfeld constant, and $C_{\rm ph}(T) = \beta T^3 + \delta T^5$ is the lattice contribution. The best fit to the $H = 500$ Oe data yields $\gamma_N = 5.92(1)$ mJ/mol K^2, $\beta = 0.191(1)$ mJ/mol K^4, and $\delta = 0.801(4)$ μJ/mol K^6. The estimated Debye temperature $\Theta_D(0) = 414(1)$ K is lower than that of CaC_6 [$\Theta_D(0) = 598$ K] as expected from the atomic mass difference. From a comparison of γ_N with the calculated density of states at the Fermi level E_F, $N(0)$, we estimate the e-ph coupling strength λ using the relation $\gamma_N = (2\pi^2 k_B^2/3)N(0)(1 + \lambda)$. With $N(0) = 1.63$ states/eV cell, we arrive at $\lambda = 0.54(1)$, somewhat lower than in CaC_6 but still in the intermediate coupling regime.

The difference ΔC_p between the normal and the superconducting states is shown in Fig. 2. At low temperatures, $\Delta C_p(T)$ exceeds the BCS prediction while it is slightly lower than the BCS value near T_c. Using the "α model," which assumes an isotropic s-wave BCS gap $\Delta(T)$ scaled by the factor $\alpha = \Delta(0)/k_B T_c$, we were able to fit the detailed temperature dependence of $\Delta C_p(T)/T$ by adjusting the gap ratio to $\alpha = 1.67$. Accordingly, the corresponding $2\Delta(0)/k_B T_c = 3.34$ is somewhat reduced below the weak coupling BCS limit of 3.52.

First, we discuss the anisotropy of the superconducting properties of SrC_6. The anisotropy of the upper critical fields $\Gamma_H = H_{c2}^{\perp}/H_{c2}^{\parallel}$ amounts to ≈ 2 at $T \sim T_c/2$, close to that of YbC_6 [1] but significantly smaller than found in CaC_6 ($\Gamma_H \sim 4$) [2]. Assuming an isotropic superconducting gap, the anisotropy Γ_H reflects the anisotropy of the Fermi velocities. Our *ab initio* calculations for the Fermi surface (FS) of CaC_6 and SrC_6 clearly reveal an elliptical sheet, associated mainly to interlayer states, and a tubular structure, of π^* character (cf. Ref. [16]). In SrC_6, the FS for the IL bands has a more pronounced 2D character and is

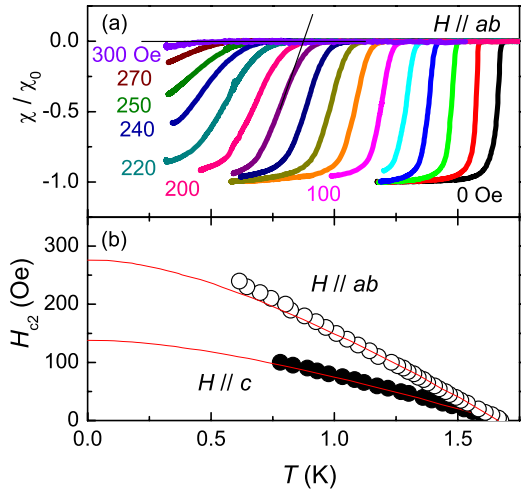

FIG. 1 (color online). (a) Temperature dependence of the normalized ac susceptibility of SrC_6 for various fields (as indicated) perpendicular to the c axis [$\chi_0 = \chi(0.3\ \text{K})$]. T_c is determined from the intersection between the extrapolated lines of the steepest slope of $\chi(T)$ and of the normal state $\chi(T)$ as shown by the solid (black) lines. (b) The $H_{c2}(T)$ for the $H \parallel ab$ plane and the $H \parallel c$ axis. The WHH curves for both H directions are shown with (red) lines.

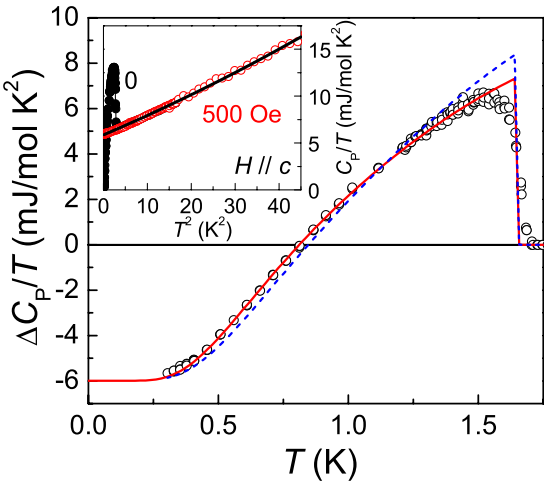

FIG. 2 (color online). Temperature dependence of $\Delta C_p/T = C_p(H = 0)/T - C_p(H = 500\ \text{Oe})/T$. The (blue) dashed and (red) solid lines represent the BCS curve and the best fit according to the α model (see text), respectively. The inset shows the temperature dependence of C_p at $H = 0$ and 500 Oe. The solid (black) line through the data points for $H = 500$ Oe is a fit to a polynomial as described in the text.

open, which results from the 10% increase of the c-axis lattice parameter as compared to CaC_6. The anisotropy of the average Fermi velocities $\Gamma_{v_F} = (\langle v^2_{F_{ab}} \rangle / \langle v^2_{F_c} \rangle)^{1/2}$ is very close in the two compounds: $\Gamma_{v_F} \approx 1.9$ in CaC_6 and ≈ 1.7 in SrC_6. If we, however, consider only the IL sheets where the superconducting gap is larger [18], we find a much larger difference: $\Gamma_{v_F} = 1.1$ for CaC_6 and $\Gamma_{v_F} = 2.1$ for SrC_6. Therefore, Γ_H of SrC_6 is expected to be larger or at least similar to that of CaC_6. The significantly enlarged anisotropy of H_{c2} in CaC_6 with respect to SrC_6 therefore cannot be understood in terms of the anisotropy of the Fermi velocities but must be attributed to an anisotropy of the superconducting gap as well.

This conclusion is supported by the reduced C_p jump observed in SrC_6. Assuming an isotropic gap, the normalized jump $\Delta C_p(T_c)/\gamma_N T_c$ grows with the e-ph coupling strength over the BCS weak coupling limit of 1.432. With $\lambda \approx 0.54$ estimated from C_p, $\Delta C_p(T_c)/\gamma_N T_c$ is expected to be enhanced over the BCS value. The experimental $\Delta C_p(T_c)/\gamma_N T_c = 1.426$, however, is *smaller* than the BCS value. As a characteristic feature of the anisotropic superconducting gap, the entropy "lost" near T_c is transferred to lower temperatures (Fig. 2) [18]. These findings indicate that the superconducting gap in CaC_6 as well as in SrC_6 has a marked anisotropy, which is also supported by recent calculations [18] showing that CaC_6 indeed exhibits a strongly **k**-dependent superconducting gap due to anisotropic e-ph interaction. Considering that the deviation of $\Delta C_p(T)$ from the predicted curve for the isotropic gap model is less pronounced for SrC_6 than for CaC_6 [17], the superconducting gap anisotropy is weaker for SrC_6. This is also consistent with the reduced anisotropy in H_{c2}. Therefore, replacing Ca with Sr decreases not only the strength of the e-ph coupling but also its anisotropy.

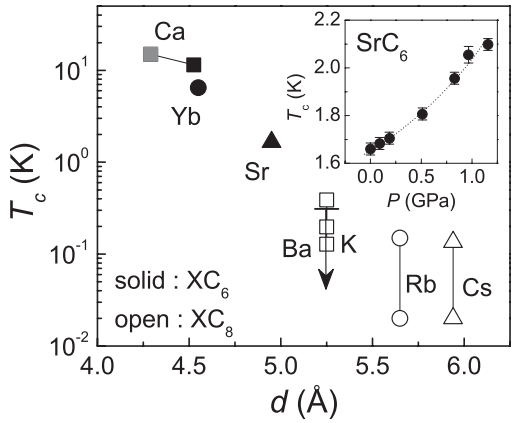

FIG. 3. T_c as a function of the graphite layer distance, d for the alkali GICs, XC_8 (X = K, Rb, and Cs), and the alkaline-earth GICs XC_6 (X = Ca, Yb, Sr, and Ba). For CaC_6, T_c at high pressure ($P = 8$ GPa) [10] is also plotted (gray square), and the graphite layer distance for the compressed CaC_6 is estimated from the theoretically calculated bulk modulus [9]. The upper limit of T_c for BaC_6 is indicated by the arrow. The inset shows T_c vs pressure for SrC_6.

We can now discuss the reduced T_c of SrC_6, which is about an order of magnitude smaller than T_c of CaC_6. When Ca is replaced with Sr, T_c decreases much more than it would be expected in the view of the alkaline-earth "isotopic" substitution [4]. With $\sqrt{M_{Sr}/M_{Ca}} \simeq 1.48$, one expects a T_c of 7.8 K for SrC_6, hence much larger than the experimental value. We thus conclude that the mass of the intercalant is not the main factor which determines T_c. Instead, we found that the T_c's of the superconducting GICs strongly depend on the graphite interlayer distance d. Figure 3 illustrates that T_c decreases rapidly, almost exponentially with increasing d for both alkali and alkaline-earth GICs [25,26]. The increase of T_c with pressure found for CaC_6 [8–10] and SrC_6 ($dT_c/dP \sim 0.35$ K/GPa, the inset in Fig. 3) clearly manifests a similar trend. We do not find any clear correlation of T_c with other structural parameters such as, e.g., the in-plane lattice constant or the distance between the adjacent intercalated atoms. We conclude that the main factor that governs the significant decrease of T_c in SrC_6 as well as the absence of superconductivity in BaC_6 down to 0.3 K is the increased distance between the graphite layers.

Figure 4 clearly demonstrates why. In the calculated phonon density of states (PhDOS) [Fig. 4(c)] and the corresponding Eliashberg functions $\alpha^2F(\omega)$ [Fig. 4(d)] for CaC_6 and SrC_6, we observe three groups of phonons: intercalant-related vibrations (I_{xy} and I_z) at $\omega \leq 20$ meV, C out-of-plane vibrations (C_z) around 50 meV, and C bond-stretching vibrations (C_{xy}) at $\omega > 150$ meV. The qualita-

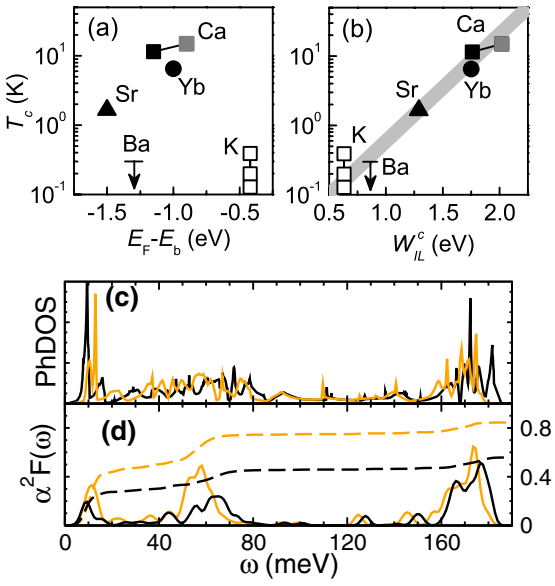

FIG. 4 (color online). (a) T_c vs the position of the bottom of the interlayer bands (E_b) with respect to E_F. (b) T_c vs the band width of the interlayer bands along the c axis (W^c_{IL}). The gray line is meant as a guide to the eye. (c) Phonon density of states and (d) Eliashberg function $\alpha^2F(\Omega)$ and frequency-dependent electron-phonon coupling $\lambda(\omega) = 2\int_0^\omega \alpha^2F(\Omega)/\Omega d\Omega$ for CaC_6 (orange) and SrC_6 (black).

tive shape of $\alpha^2F(\omega)$ is the same in the two compounds, indicating a similar spectral distribution of the e-ph interaction. But the total λ decreases from 0.83 in CaC_6 to 0.56 in SrC_6, while the logarithmic-averaged phonon frequency ($\omega_{\ln}$) remains unchanged at $\sim$305 K. The results are in very good agreement with the previous calculations for SrC_6 with the $\alpha\beta\gamma$ stacking [16]. Within computational accuracy, the difference between the $\alpha\beta$ and $\alpha\beta\gamma$ stackings seems negligible in contrast to a previous conjecture [4]. Using the Allen-Dynes formula, with $\mu^* = 0.145$, we obtain $T_c = 11.4$ K for CaC_6 and $T_c = 3.1$ K for SrC_6, in reasonable agreement with the experimental results and previous calculations [16].

The reduction of T_c in SrC_6 is due to the simultaneous decrease of the I_{xy} and C_z contribution to the e-ph coupling. The reduced coupling for the low-lying I_{xy} vibrations has a negative effect on T_c, but it is also very effective in increasing $\omega_{\ln}$; thus, the effect is partly compensated. On the other hand, the large reduction of coupling associated to C_z vibrations, which happens at energy scales comparable to $\omega_{\ln}$, reduces λ, leaving $\omega_{\ln}$ unchanged, and has a large effect on T_c. The reduction of e-ph coupling for C_z vibrations in the intermediate energy range is essential to explain the significantly lower T_c for SrC_6 than CaC_6.

The e-ph interaction for the C_z modes, and to a lesser extent for the I_{xy} ones, is associated to the interband coupling between the IL and π^* states [27]. Going from CaC_6 to SrC_6, this interband coupling is essentially reduced by the increase of the c-axis lattice constant, which decreases the real-space overlap between IL and π^* wave functions. The characteristic parameter monitoring the IL-π^* overlap is the bandwidth of the IL band along the c axis (W^c_{IL}). Figure 4(b) demonstrates that T_c for both alkali and alkaline-earth GICs is directly correlated to W^c_{IL}, clearly explaining the T_c dependence on the graphite layer distance. This observation is in strong contrast to the dependence of T_c on the degree of filling for the IL band [Fig. 4(a)]. Even though this band has to be occupied for superconductivity to occur [3], there is no clear correlation of T_c with the number of IL electrons.

Our findings indicate that C phonon modes play a nontrivial role in the superconductivity of the GICs, in contrast with the conjecture from the Ca isotope experiments [12]. Since C would give a sizable contribution to the isotope effect, the total isotope exponent would exceed the BCS limit $\alpha_{T_c} = 0.5$, which requires further studies on the effects of C isotope substitution.

In conclusion, we reported that SrC_6 becomes superconducting at $T_c = 1.65(6)$ K, but BaC_6 stays normal, conducting down to 0.3 K. The reduced C_p jump at T_c in SrC_6 and the reduced anisotropy H_{c2} in comparison with the corresponding data for CaC_6 strongly support the idea of an anisotropic superconducting gap [17,18]. We give clear evidence that T_c of the GICs essentially depends on the graphite layer distance due to sensitive change of e-ph coupling for *both* in-plane intercalant and the out-of-plane C phonon modes. Our results suggest that a possible route to increase T_c is to replace Ca by smaller atoms, such as Mg. Several attempts to prepare pure MgC_6 have failed so far, but partial substitution of Mg or Li, as long as the filling of the IL bands is kept, could be possible to reduce d, stabilize the structure, and, as a result, increase T_c.

The authors acknowledge useful discussions with A. Simon, O. K. Andersen, G. B. Bachelet, M. Giantomassi, and D. Guerald, and we thank E. Brücher and S. Höhn for experimental assistance.

[1] T. E. Weller, M. Ellerby, S. S. Saxena, R. P. Smith, and N. T. Skipper, Nature Phys. **1**, 39 (2005).
[2] N. Emery *et al.*, Phys. Rev. Lett. **95**, 087003 (2005).
[3] G. Csányi, P. B. Littlewood, A. H. Nevidomskyy, C. J. Pickard, and B. D. Simons, Nature Phys. **1**, 42 (2005).
[4] I. I. Mazin, Phys. Rev. Lett. **95**, 227001 (2005).
[5] M. Calandra and F. Mauri, Phys. Rev. Lett. **95**, 237002 (2005).
[6] G. Lamura *et al.*, Phys. Rev. Lett. **96**, 107008 (2006).
[7] J. S. Kim, R. K. Kremer, L. Boeri, and F. S. Razavi, Phys. Rev. Lett. **96**, 217002 (2006).
[8] R. P. Smith *et al.*, Phys. Rev. B **74**, 024505 (2006).
[9] J. S. Kim, L. Boeri, R. K. Kremer, and F. S. Razavi, Phys. Rev. B **74**, 214513 (2006).
[10] A. Gauzzi *et al.*, Phys. Rev. Lett. **98**, 067002 (2007).
[11] N. Bergeal *et al.*, Phys. Rev. Lett. **97**, 077003 (2006).
[12] D. G. Hinks, D. Rosenmann, H. Claus, M. S. Bailey, and J. D. Jorgensen, Phys. Rev. B **75**, 014509 (2007).
[13] S. Sanfilippo *et al.*, Phys. Rev. B **61**, R3800 (2000); G. Satta, G. Profeta, F. Bernardini, A. Continenza, and S. Massidda, *ibid.* **64**, 104507 (2001).
[14] I. I. Mazin and D. A. Papaconstantopoulos, Phys. Rev. B **69**, 180512(R) (2004); M. Giantomassi, L. Boeri, and G. B. Bachelet, *ibid.* **72**, 224512 (2005).
[15] A. N. Kolmogorov and S. Curtarolo, Phys. Rev. B **73**, 180501(R) (2006); A. Y. Liu and I. I. Mazin, *ibid.* **75**, 064510 (2007).
[16] M. Calandra and F. Mauri, Phys. Rev. B **74**, 094507 (2006).
[17] I. I. Mazin *et al.*, cond-mat/0606404.
[18] A. Sanna *et al.*, Phys. Rev. B **75**, 020511(R) (2007).
[19] D. Guerard, M. Chaabouni, P. Lagrange, M. El Makrini, and A. Hérold, Carbon **18**, 257 (1980).
[20] S. Baroni *et al.*, http://www.pwscf.org.
[21] For computational details, see Ref. [9]. For Sr, we used an ultrasoft [22] pseudopotential, with semicore s and p states treated as valence.
[22] D. Vanderbilt, Phys. Rev. B **41**, R7892 (1990).
[23] N. R. Werthammer, E. Helfand, and P. C. Hohenberg, Phys. Rev. **147**, 295 (1966).
[24] Y. Koike, H. Suematsu, K. Higuchi, and S. Tanuma, Physica (Amsterdam) **99B+C**, 503 (1980).
[25] M. S. Dresselhaus and G. Dresselhaus, Adv. Phys. **51**, 1 (2002).
[26] Here we do not consider the metal-rich GICs synthesized under high pressures such as LiC_2 which are known to be *metastable*.
[27] L. Boeri, G. B. Bachelet, M. Giantomassi, and O. K. Andersen, cond-mat/0701347.